Spring 2016

Construction of Polyurethane Fabric Nanocomposites for use in Resistance Temperature Detectors-Effect of Polyurethane Concentration, Multi-Walled Carbon Nanotubes, and Oxidant

Jordan M. Shaffer
University of Akron, jms365@zips.uakron.edu

Construction of Polyurethane Fabric Nanocomposites for use in Resistance Temperature Detectors-Effect of Polyurethane Concentration, Multi-Walled Carbon Nanotubes, and Oxidant

Jordan Shaffer
The Department of Chemical Engineering

Honors Research Project

Submitted to

The Honors College

Approved:	Accepted:
_____ Date _____	_____ Date _____
Honors Project Sponsor (signed)	Department Head (signed)
Dr. Chelsea Monty	Dr. Michael Cheung
Honors Project Sponsor (printed)	Department Head (printed)
_____ Date _____	_____ Date _____
Reader (signed)	Honors Faculty Advisor (signed)
Dr. Ed Evans	_____
Reader (printed)	Honors Faculty Advisor (printed)
_____ Date _____	_____ Date _____
Reader (signed)	Dean, Honors College
Dr. Gang Cheng	
Reader (printed)	

Executive Summary

The purpose of this honors project is to create and test polymer scaffold composites to be used in resistance temperature detectors (RTDs). These RTDs can help advance temperature readings in exercise equipment, prosthetic sockets, or any other application where temperature measurements must be taken in close contact to the skin. RTDs utilize the relationship of resistance and temperature and are usually made out of highly conductive metals such as platinum, copper, or nickel. The metal RTDs pose an issue however. Metal RTDs are currently very rigid and imposes a pressure point with the body creating discomfort for the user. This project provides a possible solution by construction of a soft and flexible RTD similar to a fabric. The fabric-like RTD can be placed in prosthetic sockets, shoes, linings or any other confined area where temperature measurements are needed. This possible solution consists of adhering multi-walled carbon nanotubes (MWCNTs) to a polymer scaffold to use as the main charge carrier in the temperature sensor. The scaffold will be electrospun from a polyurethane solution with tetrahydrofuran (THF) and N, N-dimethylformamide (DMF) as the solvents. The effect of manipulating polymer concentration, MWCNT loading, oxidant type, and oxidant concentration on the temperature and resistance readings will be discussed and analyzed. This is the second part of the design of experiment. The first part was done last year and used nylon-6 as the polymer scaffold instead of polyurethane.

Sensor labeled 31-1 returned the best results of all of the sensors constructed and tested. When tested, it produced a linear current vs. potential curve, displayed good responses to temperature, and had the least amount of drift and the lowest hysteresis of all the sensors tested. A model was fitted to the data to predict the temperature from the resistance. The model was then compared to the actual data from the sensor 31-1. When compared, the model differed by

1.3ºC with a standard error of 0.65ºC. The resistance drift and percent hysteresis associated with this sensor were 0.05 ohms and 4%, respectively. The slope of the actual temperature vs. theoretical temperature returned a y-intercept not equal to zero which shows that the model does not produce a 1:1 relationship with the actual temperature data. The electrospinning process was analyzed qualitatively. The difficulty of electrospinning polyurethane is much higher than nylon-6. This project was done with a TMF:DMF ratio of 3:1. After many complications in creating consistently sufficient material, it has been concluded that in order to take this project further, adjustments to this ratio should be made. More detail surrounding this is discussed in the report.

Throughout this project a plethora of skills were gained. The most impactful skill of any research is gaining experience in a lab setting. Lab skills such as following a design of experiment, going through testing procedures, following lab safety rules, and learning how to use technical equipment only seen in a research lab were just a few of the skills obtained. Even if research is not directly applicable to employment after graduation, it helps to build a resume and give exposure to up and coming technological advancements. The lab and research experience because of this project has improved confidence with fragile equipment and improved safety awareness when working with harmful chemicals. The result of this project could be another stepping stone on the way to a flexible fabric-like temperature sensor that the market currently does not have. Impacts on society include the prosthetic, exercise, and medical fields.

Going further, research on the electrospinning of polyurethane should be completed. The solution is much more viscous than nylon-6 and beading occurs frequently during the electrospinning process. The hypothesis is that the solvents are evaporating too quickly, resulting in a higher concentration of polymer solution and thus, a higher viscosity. After the project concluded, material was made with a solvent ratio of 1:1 and is still being tested to determine the

effect of that change. Along with the electrospinning process, further research must be done to determine the reason behind why the multi-walled carbon nanotubes are clumping together rather than coating the polymer fibers after the vacuum filtration is completed.

This paper is dedicated to Nathaniel Blasdel who lost his life in the summer of 2015. He served as a mentor on this project and a friend in life. He is greatly missed.

I. Introduction

This honors design research project has been done with the purpose of creating polyurethane scaffolds to be used in the construction of resistance temperature detectors (RTDs). These RTDs will be used to detect temperature in hard to reach areas in industries related to exercise technology, prosthetics, and numerous other medical applications. Currently, RTDs are rigid and pressure points occur when used in confined areas like the inside of a prosthetic leg. The RTD produced using a polymer scaffold would be flexible and have a fabric like feel to it. It would not have any pressure points and allow the user to wear it for long periods of time with no discomfort. This project explored and analyzed the possibility of whether a polyurethane material functionalized with multi-walled carbon nanotubes (MWCNTs) and polymerized by polypyrrole (Ppy) can be the flexible RTD that the market is calling for. The polyurethane is made using an electrospinning process. The concentration of the polymer solution, the amount of multi-walled carbon nanotubes adhered to the polyurethane, and the oxidant will be manipulated to determine whether polyurethane is a suitable and reliable measuring device for temperature.

This is the second part of a previous design of experiment. The first section of the DOE analyzed and manipulated the same parameters, but a nylon-6 scaffold was used. Contributions were made to the first part, but larger and more significant contributions were made to this portion of the project. Data and results will be compared to the first part, but this report will not go into much detail about nylon-6. This work focuses on the development of an electrospinning procedure capable of producing electrospun polyurethane fiber mats with high enough quality to be used in the RTDs. Work is still being done on the in depth RTD analysis of polyurethane, but reportable data will be presented and discussed throughout this paper.

II. Background

A. Electrospinning

The electrospinning process has been around long before polymer fabrics were being used in medical and biological devices. William Gilbert was the first to discover the electrostatic connection of a liquid in the 1600s. From there, significant advancements were made in the electrospinning field. Those included published work on the behavior of fluids under electrostatic forces by John Zeleny in 1914, patents pertaining to electrospinning by Anton Formhals between 1931 and 1944, the mathematical model known as the Taylor Cone to describe the droplet effect when the solution undergoes electrostatic force, and in the 1990s the name "electrospinning" was finally coined by the Reneker research group [1]. The electrospinning of polymer solutions involves the stretching of the viscoelastic solution by a strong electrostatic field creating material with nanoscale fiber formation [2]. The electrospun fiber has a high specific surface area and a small pore size allowing for use in a variety of applications including catalysis, hydrogen fuel cells, tissue engineering, drug delivery systems, and medical related devices like the one discussed in this paper [2].

In the electrospinning process, there are parameters that affect the quality of the polymer fabric and the diameter of the nanofibers in the fabric. These parameters include viscosity of the spinning solution, weight percent concentration, applied voltage, distance between needle tip and collector, flow rate of solution through the needle, relative humidity, and temperature [3]. All of these parameters were taken into account for this project. Depending on the polymer that is being spun, different parameters will have more of an effect than others. In this paper, the electrospinning of nylon-6 and polyurethane is discussed. From previous experience, the lab group of Dr. Chelsea Monty has had success in the electrospinning and scaffold analysis of

nylon-6. Nylon-6 was used in the construction of an ion sensor for the quantification of sodium in sweat. This sensor was produced with hopes of being used in the medical field to provide a flexible point of care ion sensor for biomedical application [4]. Along with the ion sensor, nylon-6 fabric was electrospun for use in the flexible RTDs that were analyzed as part of the first portion of this DOE. Previous literature has shown that the electrospinning of polyurethane is not straightforward. With the use of tertrahydrofuran (THF) and dimethylformamide (DMF) as the solvents for polyurethane, evaporation of these organics, specifically THF, can occur. This evaporation makes it difficult to keep a constant solution concentration between when the solution is made and the time the electrospinning is done [3]. As the weight concentration increases, the viscosity also increases and can lead to beading on the collector or a plugged needle [3].

B. Resistance Temperature Detectors

Resistance temperature detectors began as a discovery of the relationship between a metal's resistance and temperature of the metal. This relationship was first discovered by Humphrey Davy at the Royal Institution in 1821. Davy stated in his paper "The most remarkable general result that I obtained… was that the conducting power of metallic bodies varied with the temperature." In the 1850s, Carl Wilhelm Siemens invented the first resistance temperature detector. He discussed the relationship of temperature and conductivity of the copper wire. The popularity of RTDs decreased after the Siemens invention, until H.L. Callendar, who explored the use of platinum as the conducting metal and filed his first patent on the resistance thermometer, reintroduced them. [5]

Resistance and temperature relationship has grown into a popular and widely used phenomenon for measuring temperature. The metals used have a high coefficient of resistivity

and the ability to maintain stability over long periods of time allowing for accurate temperature measurements. The relationship between resistance and temperature is described by equation (1) below.

$$(1) \quad R_T = R_0(1 + AT + BT^2 + CT^3 + ... + X_n T^n)$$

In equation (1), R_T is the resistance at T (^oC) and R_0 is the resistance at 0 ^oC. The constants A,B, and C are dependent on the RTD material being used. The equation can be simplified to equation (2) when milliKelvin accuracy is not required of the RTD.

$$(2) \quad R_T = R_0(1 + \alpha T)$$

In equation (2), the "A" becomes alpha (α) and this constant is known as the temperature coefficient of resistance (TCR) of a material. Due to metal's rigidity and geometrical constraints, research has been done as of late with carbon nanotubes (CNT) as temperature sensors. CNTs have high thermal stability, high thermal and electrical conductivity, and a large specific area (similar to electrospun fibers). Multi-walled carbon nanotubes are utilized in the RTDs by adhering them to the electrospun polymer material, and are used as the main charge carrier in the RTD. The nanocomposite material of the polymer and MWCNTs is functionalized with polypyrrole (Ppy). Polypyrrole is common in polymer based sensors and acts as a connection between the carbon nanotubes and the polymer. In order for the polypyrrole to functionalize the polymer, an oxidizing agent must provide sites for this to occur. Oxidants of ammonium persulfate (APS) and iron (III) chloride ($FeCl_3$) are used in this project. Table 1 displays the results of carbon nanotube sensors from literature and the alpha (TCR) values, resistance range, and temperature range associated with those sensors. [6]

Table 1: *Various carbon nanotubes and the alpha value (Temperature coefficient of resistance, TCR), the resistance range, and the temperature range associated with those sensors.[7]*

Description	Reported TCR (%/°C)	*~ΔR Range (kOhms)	**ΔT Range (°C)	Reference
MWCNTs dispersed in SEBS, drop cast onto gold electrodes on polyimide	-2.8	3 to 4	20 to 60	Matzeu et al., 2012
MWCNT powder deposited on adhesive elastic polymer between Al foil electrodes	-1.26	11 to 8	20 to 70	Karimov et al., 2012
SWCNTs dielectrophoretically bundled between Cr/Au//parylene C//Cr/Au stacked electrodes, encapsulated in parylene C	-0.57	0.0432 to 0.0295	25 to 65	Selvarasah et al., 2007
MWCNTs dispersed in PVBC_Et_3N and sandwiched between Al plate electrodes	-0.4	95.0 to 92.6	20 to 40	Giuliani et al., 2014
SWCNT network spray deposited between Cr/Au interdigitated electrodes	-0.2954	***8.4516 to 6.4232	0 to 80	Cagatay et al., 2014
MWCNT powder deposited and pressed on glue on paper with silver paste electrodes	-0.24	0.115 to 0.096	20 to 75	Karimov et al., 2011
MWCNT dispersion vacuum filtered over nylon 6 nanofiber membrane with PPy overcoat	-0.204	6.6 to 6.85	25 to 45	Blasdel et al., 2015
MWCNTs dielectrophoretically bundled between Cr/Au electrodes, encapsulated in parylene C	-0.18	97 to 91	25 to 60	Fung and Li, 2004
MWCNTs dispersed in PMMA paste, dried onto yarn fiber, and encapsulated in thin silicon paste	-0.13	320.75 to 317.53	30 to 45	Sibinski et al., 2010
MWCNTs ODEP assisted self assembly between Au electrodes on hydrogenated amorphous silicon on ITO glass	-0.109	840 to 770	26 to 102	Hsu and Lee, 2014
Solvent assisted capillary self-assembly of microbridge made from CCVD grown MWCNTs on TiN electrodes	-0.1	1.43 to 1.22	27 to 147	De Volder et al., 2010
MWCNTs grown by CCVD on Co/Fe-Al_2O_3 from ethylene in helium, dispersed and vacuum filtered over a membrane and removed as variable thickness freestanding films	-0.08	1.15 to 0.94	-123 to 177	Di Bartolomeo et al., 2009
Graphene Nano Platelets (GNPs) drop cast onto silver paste/silicon rubber IDE on polyimide sheet	0.0371	125 to 500	10 to 60	Tian et al., 2014
PECVD CNTs grown on Y:Fe catalyst sol-gel spin coated onto silicon	0.0421	2.5 to 25	20 to 150	Ali and Hafez., 2013
Long SWNT (10's of μm) array grown between Cr/Pt electrodes on silicon by CCVD of EtOH and $FeCl_3$	0.601	1150 to 2500	0 to 100	Yang et al., 2010
Metallic SWNT CMOS compatible between Pt electrodes on SiO_2	0.9	7 to 25	20 to 400	Mohsin et al., 2014

*Most usually read from the graph and not explicitly stated throughout the text

**Most usually explicitly stated in the text, but sometimes taken from the the graph when best suited

***Calculated based on tabulated R_0 values and % changes from the graph

III. Experimental Methods

A. Design of Experiment

This research project report as stated before is only half of the original DOE. Table 2 displays the second half of the DOE that this report discusses. Runs 1-18 pertain to the nylon-6 material and were done previously. Only runs 19-36 will be looked at for this report. A previous honors research report discusses in detail the work done with the nylon-6 material in RTDs [8]. It is a Taguchi L36 DOE consisting of five factors. Each run will have a duplicate (19-1 and 19-2) to check repeatability of the testing. The polymer type is polyurethane (PU), the polymer concentration is in weight percent (wt%), the MWCNT loading is in milligrams (mg), and the oxidant concentration is in millimolar (mM).

Table 2: *Second portion of the full design of experiment for resistance temperature detectors project.*

Run	Polymer Type	Polymer Conc. (wt%)	MWCNT Loading (mg)	Oxidant Type	Oxidant Conc. (mM)
19	PU	8	2.1	APS	50
20	PU	10	2.3	APS	75
21	PU	12	1.9	APS	100
22	PU	8	2.1	APS	75
23	PU	10	2.3	APS	100
24	PU	12	1.9	APS	50
25	PU	8	2.3	APS	75
26	PU	10	1.9	APS	100
27	PU	12	2.1	APS	50
28	PU	8	2.3	$FeCl_3$	75
29	PU	10	1.9	$FeCl_3$	100
30	PU	12	2.1	$FeCl_3$	50
31	PU	8	2.3	$FeCl_3$	100
32	PU	10	1.9	$FeCl_3$	50
33	PU	12	2.1	$FeCl_3$	75
34	PU	8	2.3	$FeCl_3$	50
35	PU	10	1.9	$FeCl_3$	75
36	PU	12	2.1	$FeCl_3$	100

B. Chemical and Materials

In this project, the chemicals were used as received from their respective suppliers and no further purification or manipulation was done to them. Polyurethane pellets were purchased from Lubrizol Corporation. Tetrahydrofuran (THF) is supplied from Sigma Aldrich and is 99.9% pure. N, N-Dimethylformamide (DMF) is supplied from Fisher Scientific and also 99.9% pure. Multi-walled carbon nanotubes were acquired from Nanostructured & Amorphous Materials Inc. with a 10-20 nanometer diameter, 0.5-2.0 micrometer in length, and 95% purity. The surfactant used was Triton X-114, obtained from Acros Organics. The oxidants ammonium persulfate (APS) was acquired from Sigma Aldrich and iron (III) chloride hexahydrate ($FeCl_3$•6 H_2O) with a purity of ≥98% from Flinn Scientific. Lastly, pyrrole was obtained from Acros Organic as well at a purity of ≥99%.

C. Electrospinning

The solution for the electrospinning process consisted of three weight percent concentrations of polyurethane at 8, 10, and 12 percent. The solvent ratio was a 3:1 ratio of THF to DMF. The composition of the three different weight percent solutions can be found in Table 3. For most data presented in this report, the solvent ratio was kept at 3:1, however, it was changed to a 1:1 ratio in recent testing discussed briefly in section "V." The solution is made up the night before the electrospinning takes place to ensure full dissolving of the polymer.

Table 3: *Composition of the polyurethane solution used in the electrospinning process.*

Polymer Wt%	THF (mL)	DMF (mL)	Polyurethane (g)
8	8.44	2.64	0.8696
10	8.44	2.64	1.111
12	8.44	2.64	1.3636

The electrospinning set-up is found in Figure 1. The polymer solution is put into the two 5 mL syringe barrels and then secured on the metering pump (Figure 1, label 1 & 2). The metering pump is kept at 5.5 microliters/minute. The solution is fed through PTFE tubing with dimensions of 1/16" ID and 1/8" OD leading to two flat tip stainless steel needles. The high voltage source is connected in parallel and set to 9 kV (Figure 1, label 3). The assembly has the ability to move the needles laterally (Figure 1, label 4). The material is spun for a 6-hour period and every two hours the needles are moved laterally to give an even distribution of spray onto the collector. The needles are placed approximately 9 cm away from the collection drum. The collection area (Figure 1, label 5) is a rotary drum running at approximately 7 revolutions/minute composing of a copper sheet covered in non-stick aluminum foil (Reynolds Brand). The non-stick foil allows for easy material separation after the spun polymer has dried. Numerous test trials were done with other materials (paper towel, plastic, regular aluminum foil), but separation of the spun polymer was difficult. The assembly has a ground wire and is displayed in Figure 1, label 6. The material was spun at room temperature, usually between 20-23ºC and the humidity was monitored and kept between 30-40%RH through the pumping of humidified air in the assembly area. This is a similar set-up to the spinning of nylon-6, however a dual needle assembly is necessary when spinning polyurethane. Figure 2 gives a closer look at this dual needle set-up with the voltage source in parallel. Also, rather than a paper towel as the collector which was used in nylon-6 spinning, non-stick aluminum foil is used as the collecting material covering the copper sheet.

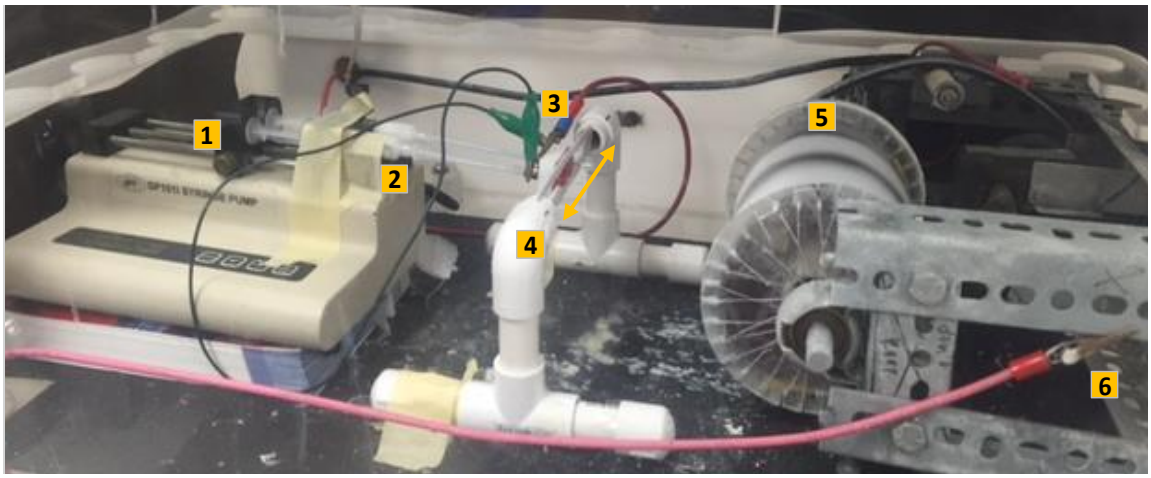

Figure 1: *Electrospinning set-up.* ***1.*** *World Precision Instruments Inc. SP101I syringe pump.* ***2.*** *Dual syringe barrel set-up dispensing polyurethane.* ***3.*** *Gamma High Voltage Research ES30P-5W voltage source connect it parallel to the dual flat tip needles.* ***4.*** *Lateral adjustment structure.* ***5.*** *Rotating drum with non-stick aluminum foil covered copper sheet.* ***6.*** *Ground connection.*

Figure 2: *A closer look at the dual needle assembly with the voltage source set-up in parallel.*

D. Functionalization of Material with MWCNTs

After the material has been spun, the non-stick aluminum foil is taken off the copper sheet and disks are cut in the polyurethane material to the approximate diameter or 47mm. The full step by step process is illustrated in Figure 3. The disks are separated from the aluminum foil and are ready for filtration. The MWCNT solution is made by taking 1.9, 2.1, or 2.3 mg of

MWCNT and mixing it with 34 mL of 0.002 M Triton X-114 solution and 216 mL of DI water. The solution is then sonicated using a Misonix Ultrasonic Processor XL on level 5 for 3 minutes. After the solution is prepared the vacuum filter is set-up by taking the polyurethane disk and a Whatman filter cut to a slightly larger diameter than the polyurethane, and placing them on the vacuum filter. Once the vacuum is turned on, take 1-2 mL of 0.002 M Triton X-114 solution and wet the membrane. The top of the funnel is put on the vacuum filter and secured with parafilm and a clamp. With the vacuum on, the assembly is tilted to a 45 degree angle and the MWCNT is poured into the top of the assembly. The vacuum is then taken to 5 inHg, and the MWCNT solution is filtered through the polyurethane material. When finished, the sensor is dried using nitrogen and placed in a desiccator. An actual photo of this filtration is found in Figure 4.

Once dry, the fabric nanocomposite is spin coated using either ammonium persulfate or iron (III) chloride at varying concentrations of 50, 75, and 100 mM. One milliliter of oxidant solution is applied in the manner presented in Figure 5. The spin coating dvice is connected to a Philmore regulating transformer set to 36-volts spinning a weigh boat with the material inside. The material is again placed in a desiccator and left overnight to dry. After it is dry, it placed in a polymerization chamber with a beaker of 1 mL of pyrrole inside. The samples were left in the chamber for 48 hours and then taken out for use in the RTD.

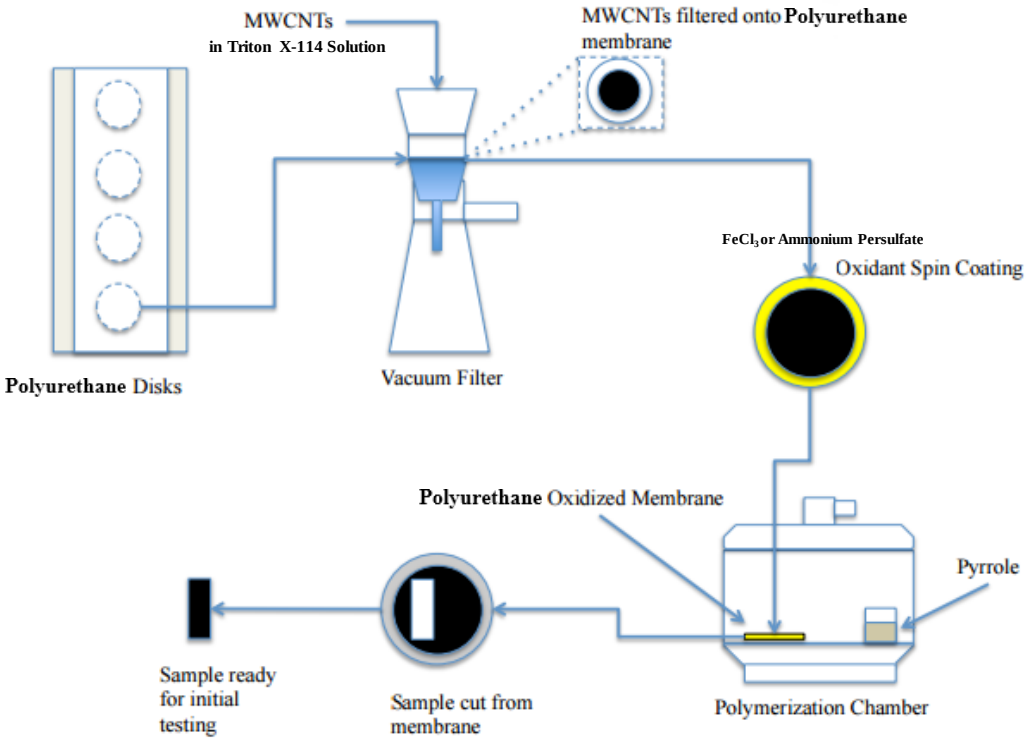

Figure 3: *Sensor construction process [8].*

Figure 4: *Vacuum filtration for the adhering of the MWCNTs. 1) 250 mL of MWCNT in Triton X-114. 2) Vacuum filtration flask. 3) Dry ice with isopropanol trap. 4) Welch Gem B290 vacuum pump. [8]*

Figure 5: *Spin coating assembly for the addition of 1 mL of oxidant.*

E. Sensor Testing

At this point the samples are ready to be constructed into a sensor and testing to determine the use of it in an RTD. Sensor testing was performed by a graduate student using a previously developed procedure [6] [8]. The data produced from the testing will be analyzed and discussed.

IV. Data and Results

A. Initial Sensor Testing

The initial sensor testing comprised of using a Cell Test system at a constant temperature of 25ºC from -700mV to 700mV. In order to move on to the second test, the sensor must return a linear IV curve. Figure 5 and Figure 7 shows a successful initial test. These are tests from the best two results, run 31-1 and 34-1. The better of the two was 31-1 and will be discussed later in the report. The linear IV curve indicates the material has gone through complete polymerization and a sufficient MWCNT network connection. Many samples failed the initial test and were repeated. Discussion of why they failed will be discussed later in the report.

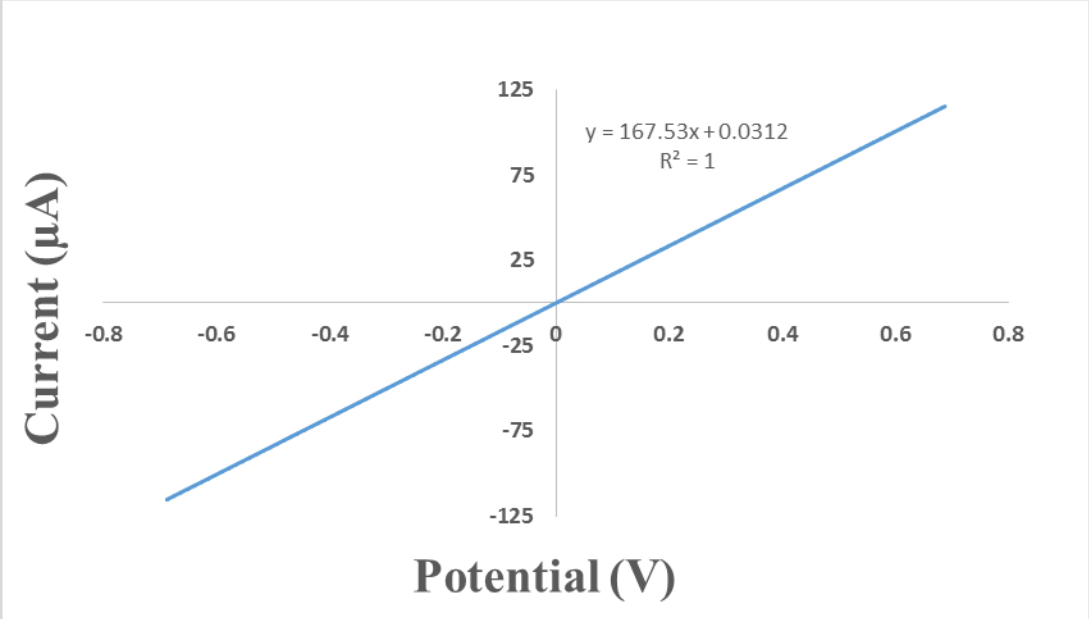

Figure 5: *Linear IV curve of sample* ***34-1*** *at constant temperature from -700mV to 700mV. The conditions of this sample were 8wt% PU, 2.3 mg MWCNT loading, and 50mM $FeCl_3$ oxidant.*

Along with an IV curve, the initial test produces a resistance vs. potential curve seen in Figures 6 and 8. The resistance is calculated using Ohm's law. A slope of 0 is ideal, but a small slope of -0.0068 and 0.0215 is a favorable result.

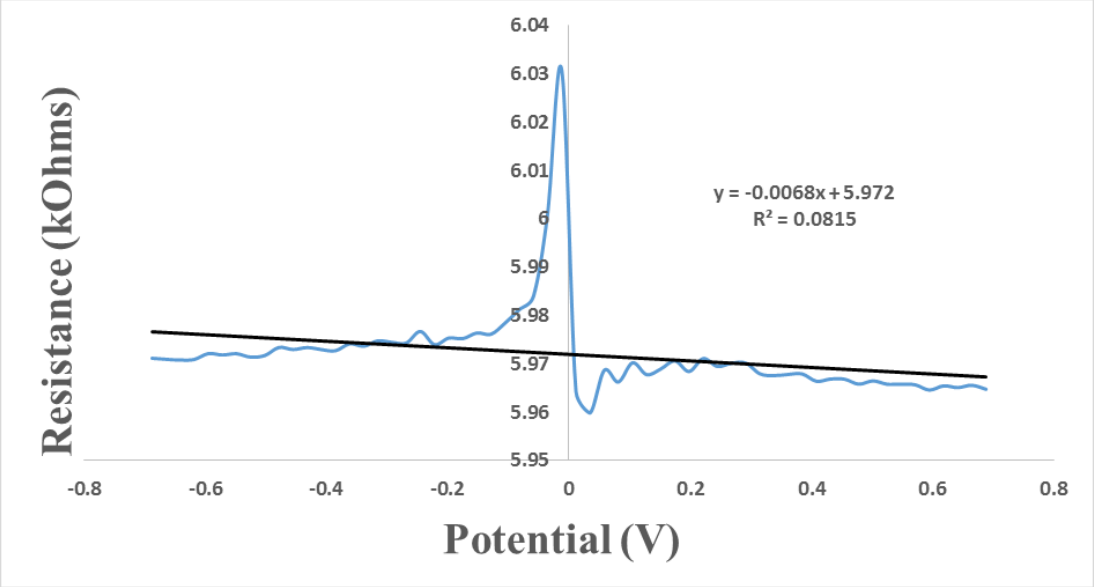

Figure 6: *Resistance curve of sample* ***34-1*** *at constant temperature from -700mV to 700mV. The conditions of this sample were 8wt% PU, 2.3 mg MWCNT loading, and 50mM $FeCl_3$ oxidant.*

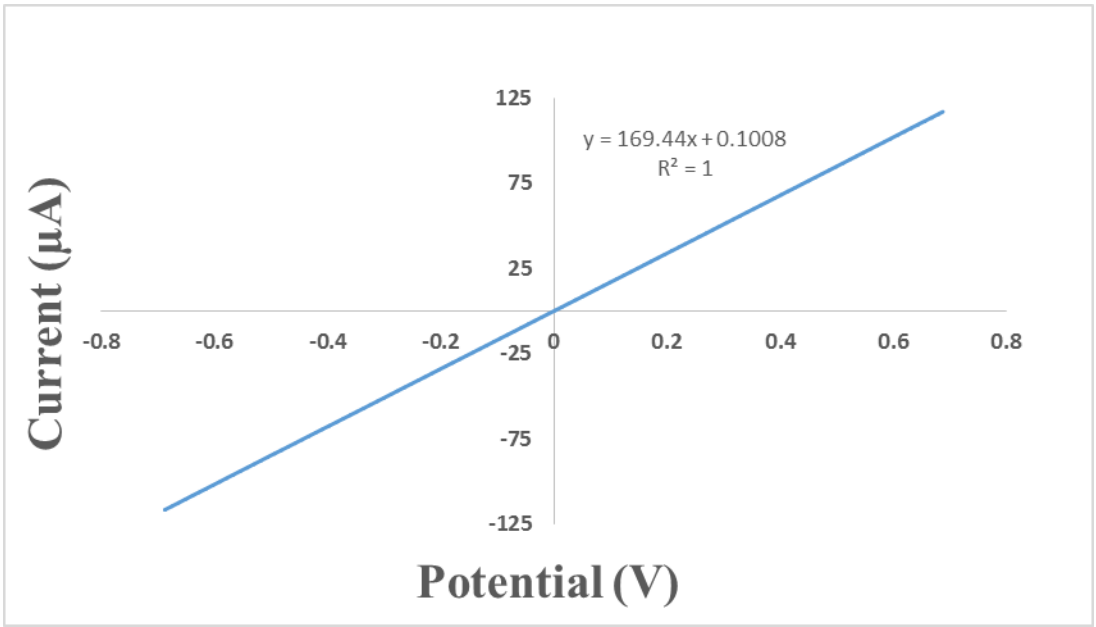

Figure 7: *Linear IV curve of sample* ***31-1*** *at constant temperature from -700mV to 700mV. The conditions of this sample were 8wt% PU, 2.3 mg MWCNT loading, and 100mM $FeCl_3$ oxidant.*

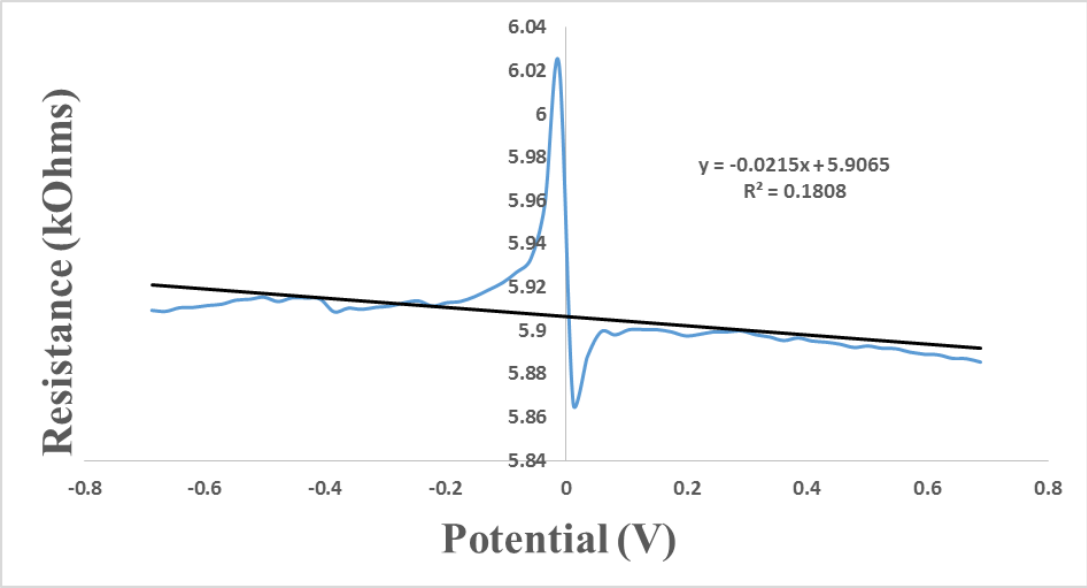

Figure 8: *Resistance curve of sample **31-1** at constant temperature from -700mV to 700mV. The conditions of this sample were 8wt% PU, 2.3 mg MWCNT loading, and 100mM $FeCl_3$ oxidant.*

B. Temperature Ramp

After the initial test, the second test was done on the sensor. A temperature ramp at a constant 700mV went from 25ºC to 45ºC and then back down to 25ºC. As seen in Figures 9 and 11, the resistance is inversely related to the temperature. As the temperature increases, the resistance decreases. Drift can occur and is defined as the difference between the initial resistance and the resistance at the end of the ramp. In Figure 9, sample 34-1 had relatively minimal drift. In Figure 10, the drift is clearly seen for sample 34-1. The best result was sample 31-1 because of how minimal the drift was. The graphs for this sample are in Figures 10 and 12.

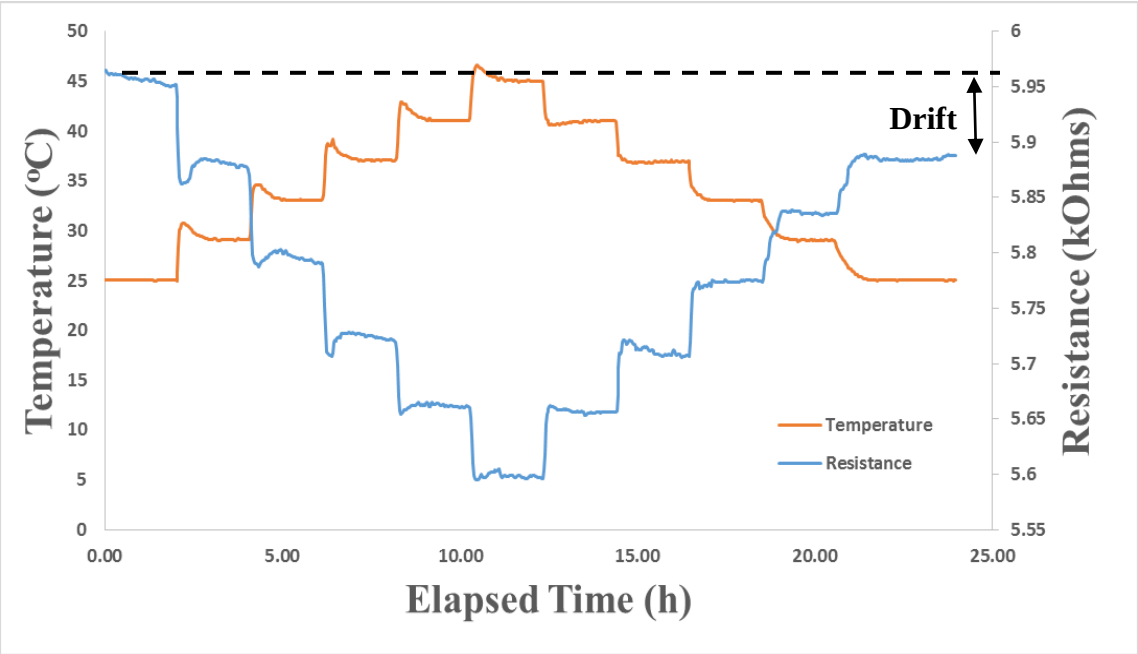

Figure 9: *Temperature ramp from 25°C to 45°C and then back to 25°C at constant 700mV of sample* ***34-1****. Temperature ramp vs. time is the orange line and resistance vs. time is the blue curve. The conditions of this sample were 8wt% PU, 2.3 mg MWCNT loading, and 50mM $FeCl_3$ oxidant.*

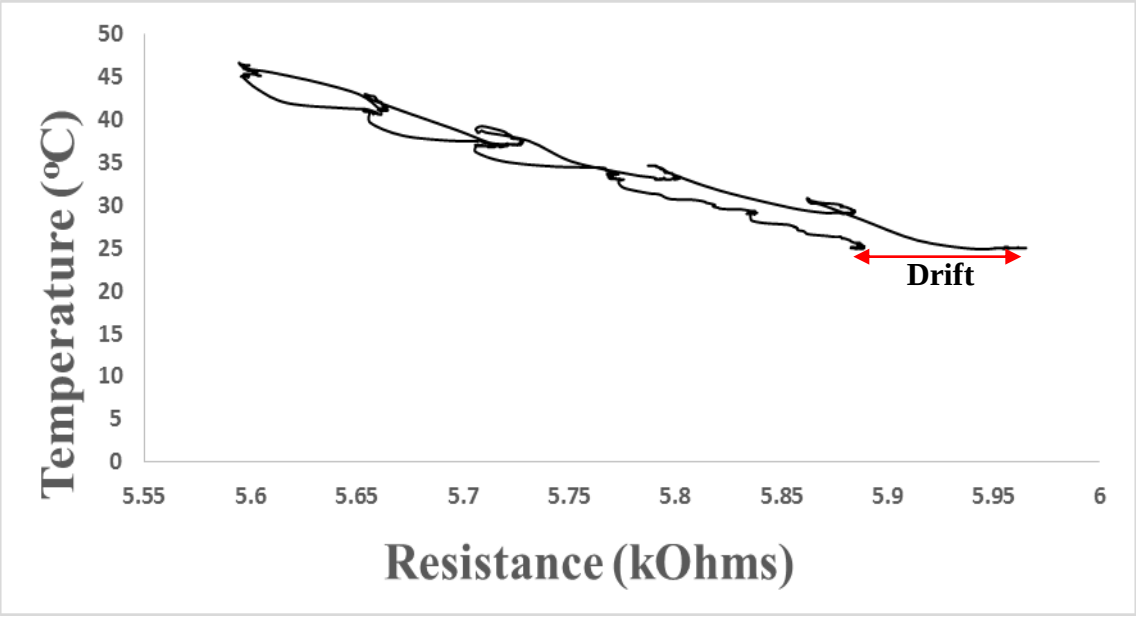

Figure 10: *Temperature/resistance graph of temperature ramp of sample* ***34-1*** *from 25°C to 45°C to 25°C at constant 700mV. The conditions of this sample were 8wt% PU, 2.3 mg MWCNT loading, and 50mM $FeCl_3$ oxidant.*

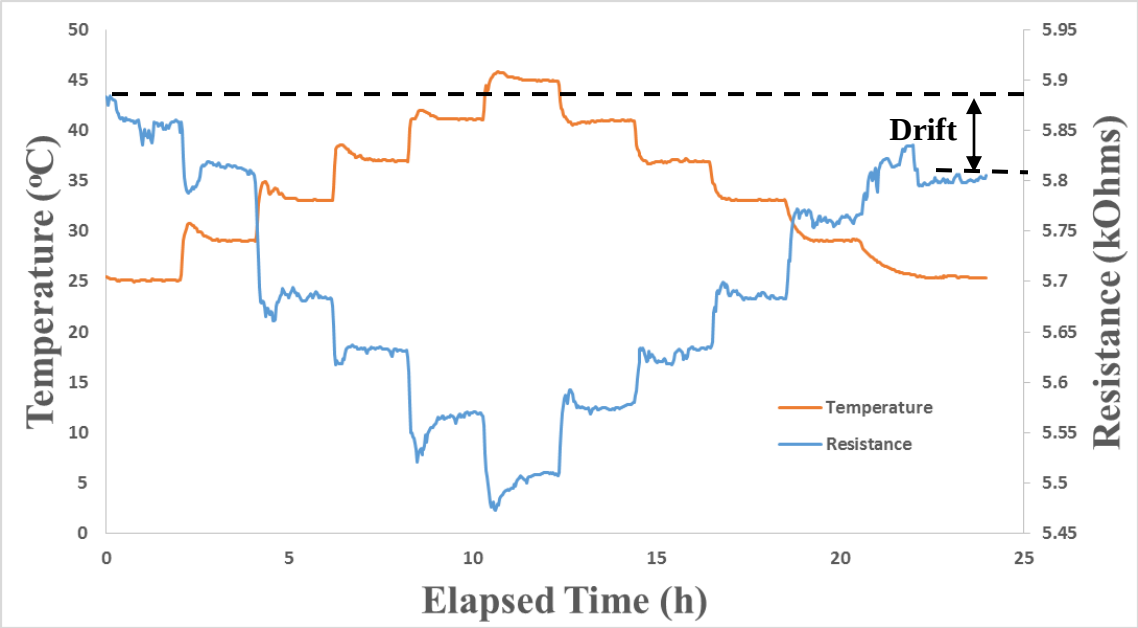

Figure 11: *Temperature/resistance graph of temperature ramp of sample* ***31-1*** *from 25°C to 45°C to 25°C at constant 700mV. The conditions of this sample were 8wt% PU, 2.3 mg MWCNT loading, and 100mM $FeCl_3$ oxidant.*

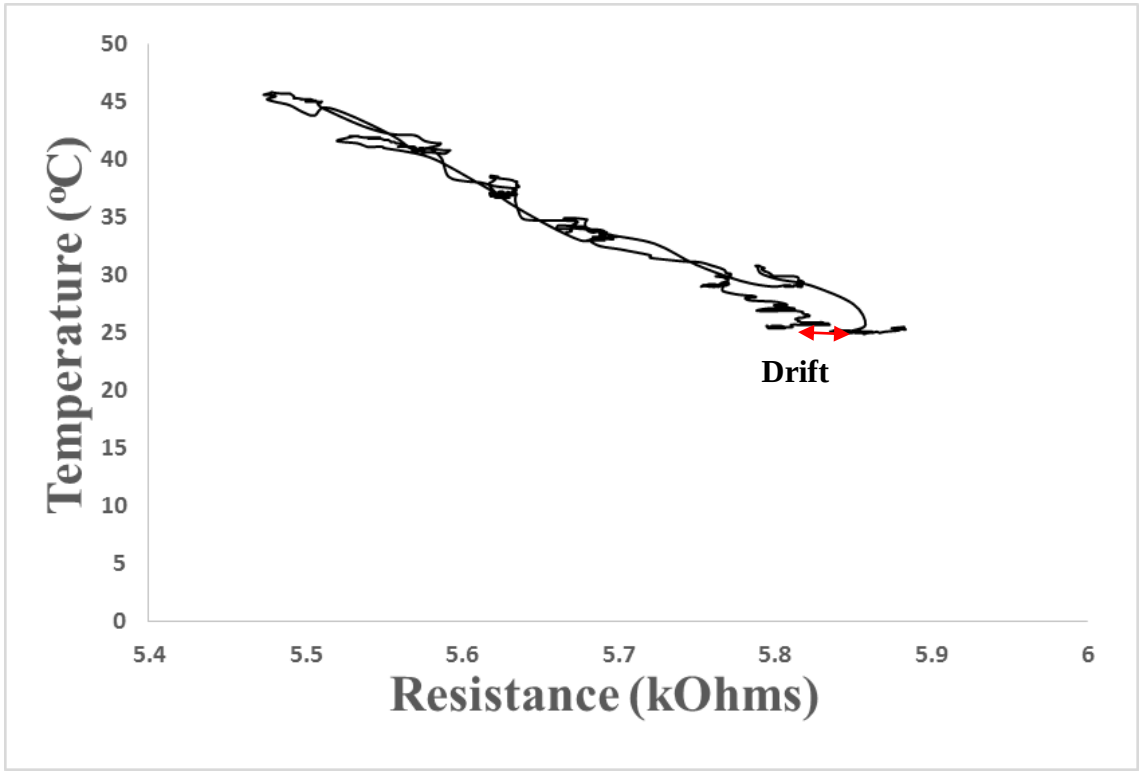

Figure 12: *Temperature/resistance graph of temperature ramp of sample* ***31-1*** *from 25°C to 45°C to 25°C at constant 700mV. The conditions of this sample were 8wt% PU, 2.3 mg MWCNT loading, and 100mM $FeCl_3$ oxidant.*

Sample 26-2 seen in Figure 13 is an example of a bad result. As the temperature is ramped, the resistance produces no response. Further analysis must be done to understand why this non-response occurred. SEM analysis and conductivity test will be conducted in the future and is outside the scope of this paper. Other sensors responded similar to this as well.

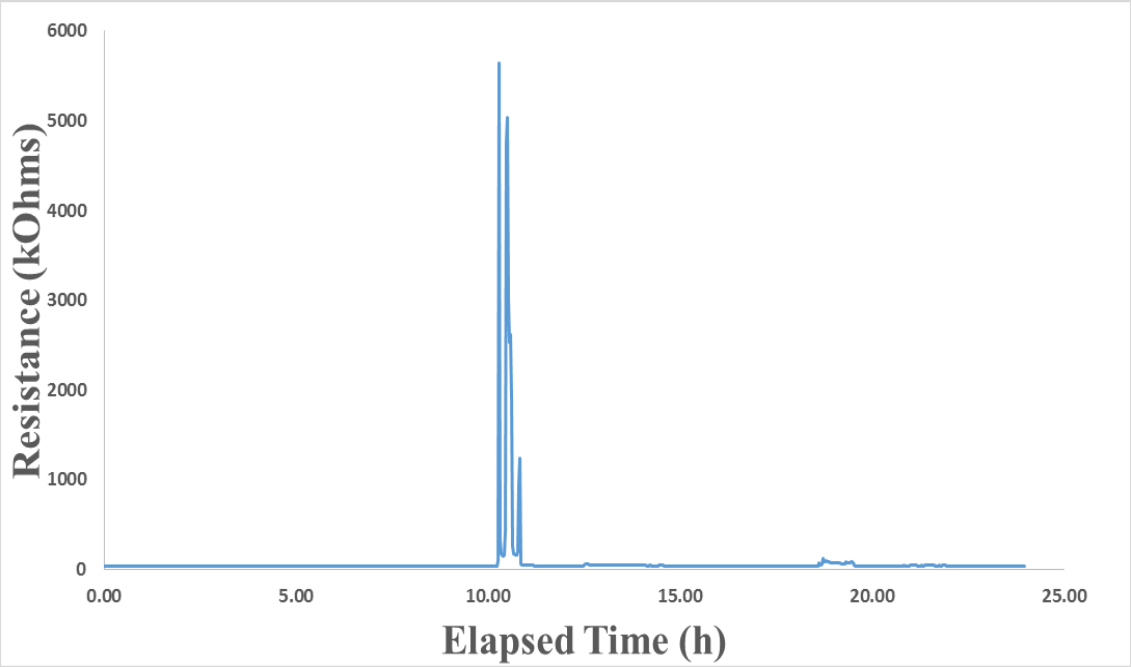

Figure 13: *Resistance graph of temperature ramp of sample* ***<u>26-2</u>*** *from 25°C to 45°C to 25°C at constant 700mV. The conditions of this sample were 10wt% PU, 1.9 mg MWCNT loading, and 100mM APS oxidant.*

V. Discussion and Analysis

A. Initial Sensor Testing

As described in the data section, the initial test was to determine whether the sensor returned a linear current vs. potential curve. Two linear graphs are displayed in Figures 5 and 7 for samples 34-1 and 31-1, respectively. The linearity test is not a tell all of whether the sensor will have success or not. The sample 26-2 returned a linear IV curve, but had no response of resistance during the temperature ramp test. The linear curve is based off of Ohm's Law (3) which produces a linear curve where the slope is the inverse of resistance 1/R.

$$(3) \quad I = \frac{V}{R}$$

Not all materials passed the initial sensor test. After the initial set of sensors were made and tested, results returned that numerous sensors failed this first test. The reason for failing this test could due to numerous reasons related to the MWCNT connection to the polymer fibers. The MWCNTs like each other more than the fiber and clumping of the nanotubes occurs. Another reason for failing the test due to a non-linear IV curve could be due to incomplete or non-uniform polymerization. If the MWCNT network does not connect to the polymer fibers, then it can act as a capacitor rather than a resistor. When compared to the nylon-6 fiber with MWCNT prior to oxidant spin coating and polymerization of the pyrrole, the polyurethane exhibits larger amount of MWCNT clumping. This can be seen in Figure 14. The MWCNT are more cohesive than adhesive and do not create the connection the way that nylon-6 does. More research is being done to understand the reasoning behind the large amount of MWCNT clumping and is not completed yet. Current hypotheses are related to fiber size being too large, or the elimination of acetone as a post filtration rinse. The acetone was used to rinse the nylon-6 sensor after the

MWCNT filtration process. However with polyurethane, the acetone was dissolving the sensor so that process was removed.

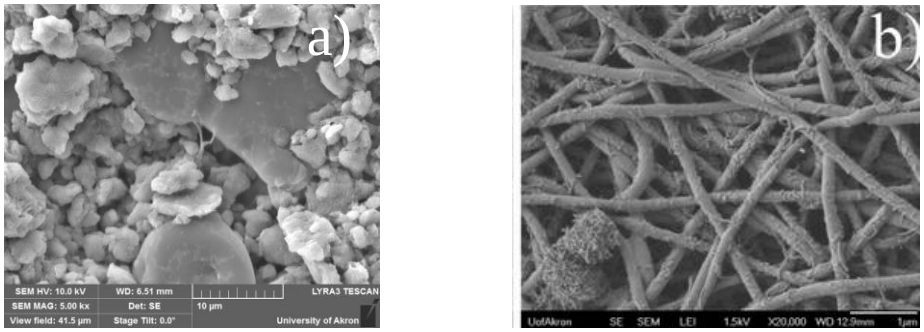

Figure 14: *SEM images of the pre-spin coated and pre-polymerized polyurethane (a) and nylon-6 (b) fibers functionalized with MWCNTs.*

B. Temperature Ramp

From the IV curves, it can predict whether the resistance will drift during the temperature ramp. It is not a tell all, but can be a good predictor. There was at least minimal drift in all of the samples tested, but sample 31-1 had the least amount of drift at 0.05 kOhms. Sample 31-1 also had little % hysteresis at approximately 4%. This is the amount of noise in the resistance response. This data is seen in Table 4. The sample 34-1 also had good results, but had a slightly higher hysteresis at 7% and a larger drift actually had less hysteresis, but had a larger drift as seen in Figures 9 and 10, and was recorded at 0.08 kOhms. The drift could be significantly reduced if an annealing process were to be applied to the sensor. After the first ramp, the drift would be reduced. From the temperature ramp, the alpha value (α) can be determined. The alpha value is known as the temperature coefficient of resistance (TCR). For sample 31-1 the alpha value is calculated to be -0.00293. The alpha value had a standard error of 0.00097. Alpha is calculated using equation (4) where R_0 is at T=25 and is 5859 ohms:

$$(4)\ \alpha = \frac{dR}{R_0 dT}$$

The temperature ramp and the alpha value can be used to develop a model that the sensor can used to determine the temperature, thus creating the resistance temperature detector. A theoretical model was produced for sample 31-1 using the alpha value of -0.00293 in the following equation (5) where T_0 is 25°C and R_0 is 5859 ohms. Table 5 displays a summary of all of the samples and the measureables associated with the initial IV test and the temperature ramp. As seen in the table, many of the polyurethane samples failed to make it passed the initial IV test.

$$(5)\ T = -\frac{1}{\alpha}\left(\frac{R}{R_0} - 1\right) + T_0$$

Table 4: *Hysteresis (%) and drift (kOhms) for sample **31-1**. The conditions of this sample were 8wt% PU, 2.3 mg MWCNT loading, and 100mM $FeCl_3$ oxidant.*

% Hysteresis	4.32%
Drift	0.05

Table 5: *Summary of all samples and the test result, notes, α-average, hysteresis (%) and drift (kOhms).*

NOTES	Run	Polymer Conc. (wt%)	MWCNT Loading	Oxidant Type	Oxidant Conc. (mM)	Drift (kOhms)	α-average	% Hysteresis
OK	19-1	8	2.1	APS	50	0.063	-3.89E-03	18.5%
OK	19-2	8	2.1	APS	50	4.550	3.01E-03	-118.8%
Bad t ramp curve	20-1	10	2.3	APS	75	2.587	-8.23E-04	81.2%
Failed	20-2	10	2.3	APS	75			
Failed	21-1	12	1.9	APS	100			
Failed	21-2	12	1.9	APS	100			
OK	22-1	8	2.1	APS	75	8.007	-2.34E-03	25.6%
Failed	22-2	8	2.1	APS	75			
OK	23-1	10	2.3	APS	100	0.338	-1.88E-03	58.4%
Failed	23-2	10	2.3	APS	100			
Failed	24-1	12	1.9	APS	50			
Failed	24-2	12	1.9	APS	50			
Failed	25-1	8	2.3	APS	75			
Failed	25-2	8	2.3	APS	75			
Failed	26-1	10	1.9	APS	100			
Failed	26-2	10	1.9	APS	100			
Failed	27-1	12	2.1	APS	50			
OK	27-2	12	2.1	APS	50	0.460	-3.81E-04	52.9%
OK	28-1	8	2.3	FeCl3	75	-0.088	-3.15E-03	-3.6%
OK	28-2	8	2.3	FeCl3	75		-4.30E-03	37.1%
OK	29-1	10	1.9	FeCl3	100	4.263	-1.46E-03	48.1%
Bad t ramp curve	29-2	10	1.9	FeCl3	100	-63.413	1.84E-02	40.5%
OK	30-1	12	2.1	FeCl3	50	-2.873	5.35E-03	-85.5%
Failed	30-2	12	2.1	FeCl3	50			
OK	31-1	8	2.3	FeCl3	100	0.051	-2.93E-03	4.3%
Failed	31-2	8	2.3	FeCl3	100			
OK	32-1	10	1.9	FeCl3	50	1.593	-2.99E-03	59.8%
Failed	32-2	10	1.9	FeCl3	50			
Failed	33-1	12	2.1	FeCl3	75			
Failed	33-2	12	2.1	FeCl3	75			
OK	34-1	8	2.3	FeCl3	50	0.077	-2.67E-03	8.0%
Failed	34-2	8	2.3	FeCl3	50			
Failed	35-1	10	1.9	FeCl3	75			
Not Found	35-2	10	1.9	FeCl3	75			
Failed	36-1	12	2.1	FeCl3	100			
Not Made	36-2	12	2.1	FeCl3	100			

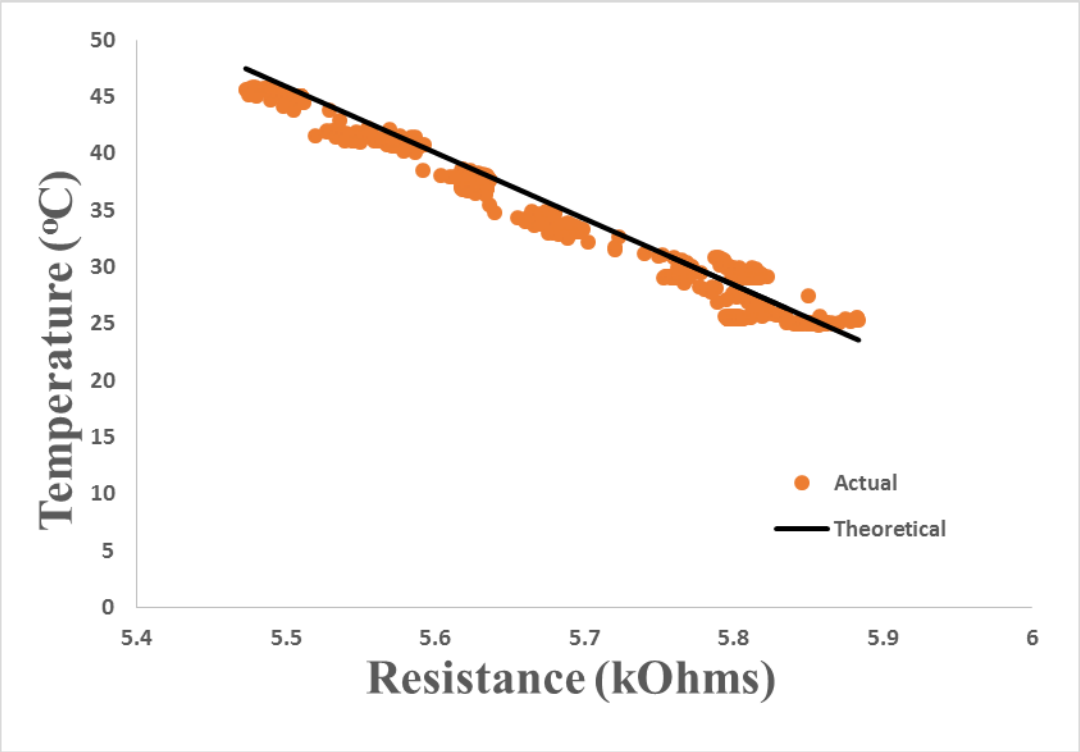

Figure 15: *Actual vs. theoretical graph of temperature and resistance relationship of sample* ***31-1****. The alpha value used was -0.00293 with standard error of 0.00097. The conditions of this sample were 8wt% PU, 2.3 mg MWCNT loading, and 100mM* $FeCl_3$ *oxidant.*

Actual data from the temperature ramp is compared to the theoretical model of equation 4 in Figure 15. The actual data follows the same trend as the theoretical data, but there is still a difference between actual and theoretical. The temperature was ramped from 25°C to 45°C and then back to 45°C with a two hour hold time at each temperature. The averages of the temperatures were taken during the hold time for both theoretical and actual. The data is displayed in Table 6. That data was then translated into a graph displaying the actual data with error bars. The error bars represent the horizontal (resistance) and the vertical (temperature) standard error of the data. That graph is shown in Figure 16. The table shows that the highest average difference is 7.6% that occurred during the last hold at 25°C with a temperature difference of 2 degrees. The average temperature difference of the data set is approximately

1.3ºC with a standard error of 0.65ºC. The average relative error is approximately 4% with standard error of 2%.

Table 6: *Temperature difference between values produced by the theoretical model and the actual measured values.*

Actual Average Hold Temperature (^{o}C)	Theoretical Average Temperature (^{o}C)	Difference (^{o}C)	Absolute Relative Error (%)
25.11	25.00	-0.11	0.43%
29.40	27.91	-1.49	5.06%
33.40	35.30	1.90	5.68%
37.34	38.30	0.96	2.57%
41.23	42.54	1.31	3.18%
33.21	35.27	2.06	6.20%
45.07	45.87	0.80	1.78%
40.95	41.44	0.50	1.21%
37.02	38.57	1.55	4.19%
29.65	31.42	1.77	5.95%
26.18	28.18	2.00	7.63%

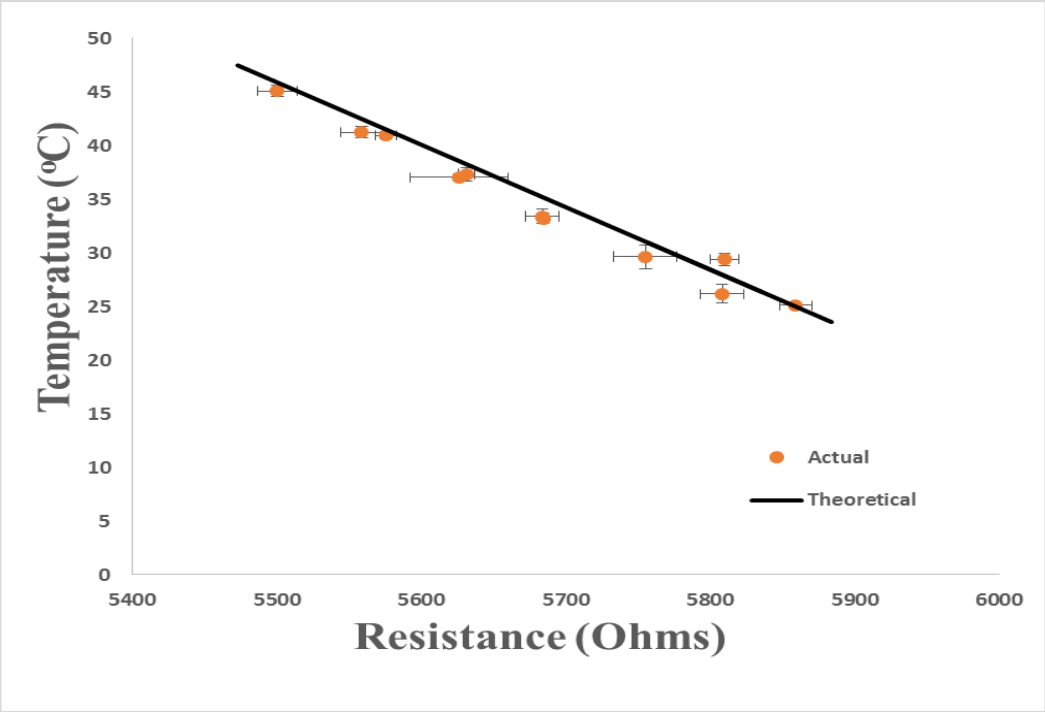

Figure 16: *Actual and theoretical temperatures corresponding to average resistances. This is for sample* ***31-1****. The conditions of this sample were 8wt% PU, 2.3 mg MWCNT loading, and 100mM $FeCl_3$ oxidant.*

Figures 15 and 16 show that there is a relationship and correlation between the theoretical model and the actual data points. The temperature from the ramp and the theoretical temperatures were graphed against each other to determine how accurate the reading would be if it were in an RTD. This graph is seen in Figure 17. The relationship has a slope slightly over 1 and the y-intercept is not equal to zero therefore showing that the actual data is not exact to the theoretical model which was already analyzed above.

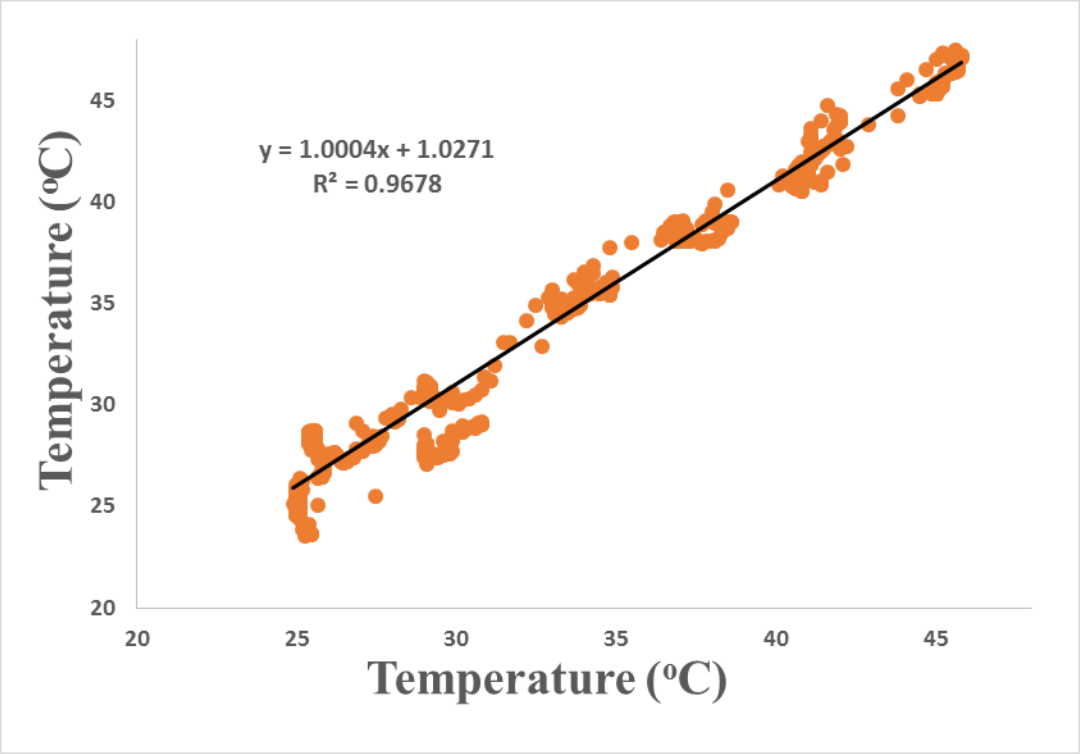

Figure 17: *Actual vs. theoretical model for predicting temperature for sample* ***31-1****. The conditions of this sample were 8wt% PU, 2.3 mg MWCNT loading, and 100mM* $FeCl_3$ *oxidant.*

C. Comparison to Nylon-6 Scaffold

As stated in this report there are much more complications with the electrospinning of polyurethane compared to nylon-6. The majority of the differences between nylon-6 and polyurethane were not quantitative, but were qualitative results. First off, during the electrospinning, the viscosity of the polyurethane was significantly higher. Even at weight percent of 8, 10, and 12 it was much more viscous then nylon-6 with weight percent of 14, 17, and 20. The higher viscosity led to a lot of beading during the electrospinning process. The best word to describe the polyurethane process is inconsistent. It seemed as though even at the exact conditions of distance, voltage, flow rate, temperature, and relative humidity the material would look great one day and awful another day. After struggling through creating sensors from the inconsistent material created, more research was done to solve the inconsistent issues. After this

project concluded, it was determined to change the THF:DMF solvent ratio from 3:1 to 1:1. The hypothesis is that the solvent is evaporating too quickly, increasing the viscosity significantly and thus creating trouble spinning. The solvent may have been evaporating between the time the solution was made and the time the solution was used to spin, or it could have occurred right as the solution gets to the needle tip. It makes sense since THF is more volatile than DMF. If the amount of THF is lowered and the evaporation is slowed down, then it seems the electrospinning will have more success.

Currently, it is still unknown as to why the polyurethane scaffold does not work as well as the nylon-6 scaffold. Future work associated with this project includes further researching and finding the ideal conditions for electrospinning polyurethane into sufficient RTD material. Contact angle testing between the MWCNTs and the polymer fibers, SEM testing, and IFM testing will be completed in future research to analyze the changing electrospinning conditions and their effect on the temperature sensors.

VI. Literature Cited

[1] Tucker, N., Stanger, J., Staiger, M., Razzaq, H., & Hofman, K. (2012). The History of the Science and Technology of Electrospinning from 1600 to 1995. *Journal Of Engineered Fibers And Fabrics*, *7*63-73.

[2] Zdraveva, E. (2011). Electrospinning of Polyurethane Nonwoven Fibrous Mats. *TEDI Međunarodni interdisciplinarni časopis*, *1*(1), 55-60.

[3] Karakas, H., Saraç, A. S., Polat, T., Budak, E. G., Bayram, S., Dag, N., & Jahangiri, S. (2013, March). Polyurethane Nanofibers Obtained By Electrospinning Process. In *Proceedings of World Academy of Science, Engineering and Technology* (No. 75, p. 607). World Academy of Science, Engineering and Technology (WASET).

[4] Wujcik, E. K., Blasdel, N. J., Trowbridge, D., & Monty, C. N. (2013). Ion Sensor for the Quantification of Sodium in Sweat Samples.*IEEE Sensors Journal*, *13*(9), 3430.

[5] L. B. Hunt, "The origin of the platinum resistance thermometer," *Platinum Metals Rev., vol. 24*, no. 3, pp. 104–112, Jul. 1980.

[6] Blasdel, Nathaniel J., Evan K. Wujcik, Joan Carletta, Kye-Shin Lee, and Chelsea N. Monty. "Fabric Nanocomposite Resistance Temperature Detector." *IEEE Sensors Journal*.

[7] Blasdel, Nathaniel J., and Chelsea N. Monty. "Temperature Sensitive Fabric for Monitoring Dermal Temperature Variations," *Wearable Electronic Sensors,* pp 193-220

[8] Howdyshell, Rebecca. "Nylon-6 Fabric Nanocomposite Resistance Temperature Detectors-Effect of Oxidant, MWCNT, and Nylon-6 Concentration." *Honors Research Project,* University of Akron Honors College.